Hindawi
Journal of Sensors
Volume 2019, Article ID 1026905, 10 pages
https://doi.org/10.1155/2019/1026905

Research Article

Performance Evaluation of Free-Space Fibre Optic Detection in a Lab-on-Chip for Microorganism

Mohd Firdaus Kamuri,[1] **Zurina Zainal Abidin**,[1] **Lee Hao Jun**,[1] **Mohd Hanif Yaacob**,[2] **Mohd Nizar Bin Hamidon**,[3] **Nurul Amziah Md Yunus**,[3] **and Suryani Kamaruddin**[1]

[1]*Department of Chemical and Environmental Engineering, Faculty of Engineering, University Putra Malaysia, Malaysia*
[2]*Department of Computer and Communications Engineering, Faculty of Engineering, University Putra Malaysia, Malaysia*
[3]*Department of Electrical and Electronic Engineering, Faculty of Engineering, University Putra Malaysia, 43400 Selangor, Malaysia*

Correspondence should be addressed to Zurina Zainal Abidin; zurina@upm.edu.my

Received 7 October 2018; Revised 5 January 2019; Accepted 30 January 2019; Published 24 March 2019

Academic Editor: Fernando Benito-Lopez

This paper describes the development of a lab-on-chip (LOC) device that can perform reliable online detection in continuous-flow systems for microorganisms. The objective of this work was to examine the performance of a fibre optic detection system integrated into a LOC device. The microfluidic system was fabricated using dry film resist (DFR), integrated with multimode fibre pigtails in the LOC. Subsequently, the performance of the fibre optic detection was evaluated by its absorbance spectra, detection limit, repeatability and reproducibility, and response time. The analysis was carried out using a constant flow rate for three different types of microorganisms which are *Escherichia coli*, *Saccharomyces cerevisiae*, and *Aeromonas hydrophila*. Under the experimental conditions used in this study, the detection limit of 1.0×10^5 cells/mL for both *A. hydrophila* and *E. coli*, while a detection limit of 1.0×10^6 cells/mL for *S. cerevisiae* cells were measured. The results also revealed that the device showed good repeatability with standard deviations less than 0.2 for *A. hydrophila* and *E. coli*, while standard deviations for *S. cerevisiae* were larger than 1.0. The response times for *A. hydrophila*, *E. coli*, and *S. cerevisiae* were 104 s, 122 s, and 78 s, respectively, although significant errors were recorded for all three species for reproducibility experiment. It was found that the device showed generally good sensitivity, with the highest sensitivity towards *S. cerevisiae*. These findings suggest that an integrated LOC device, with embedded multimode fibre pigtails, can be a reliable instrument for microorganism detection.

1. Introduction

In recent years, there has been an increasing interest in lab-s-on-a-chip (LOC) due to their versatility, ease of fabrication, and a multitude of applications in biosensing and analysis [1]. LOC have emerged as powerful platforms for detection of protein [2], nucleic acids [3], drugs [4, 5], and hormones [6, 7]. LOC devices are very promising for health monitoring, detection of pollutants, environmental studies, and point-of-care (POC) clinical. The application of LOC devices to biology and medicine has significant impacts on a variety of new research directions [8–10]. LOC devices can allow efficient in-field detection; access to sophisticated laboratories is limited, expensive, and time-consuming [1]. Additionally, the device is a portable, user-friendly miniaturised device for on-site chemical analysis and useful in the medical technology field [11]. Furthermore, the device offers a way for greater throughput with higher sensitivity and resolution [12].

Various methodologies of LOC fabrication have been widely adopted involving materials such as paper [13], glass [14, 15], polymers [16, 17], and ceramic [18, 19]. The material chosen depends on the application, physicochemical properties of the analyte, biocompatibility, and possibly integration with other devices and materials [16]. One of the approaches in LOC development is dry film resist (DFR) where it is effective, reproducible, and cheap; has a less complicated fabrication process; and is easy to handle [20].

Microfluidic technology was employed in microanalytical methods to achieve measurements or results of high sensitivity and high resolution. Its ability to be integrated with various novel detection techniques has made it versatile

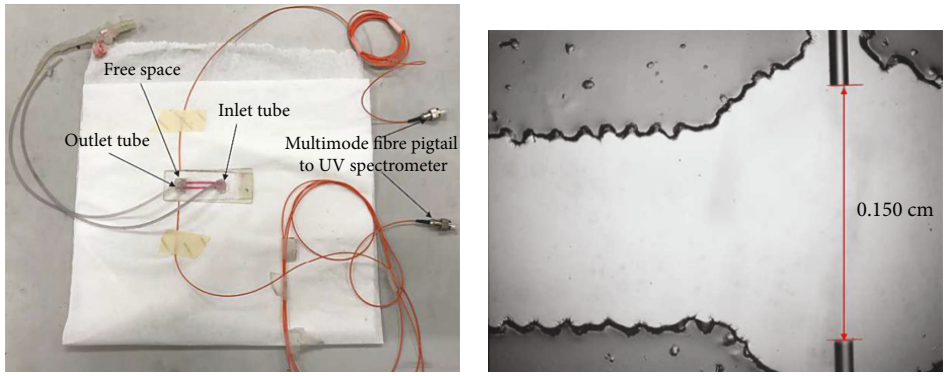

(a) (b)

Figure 1: (a) The fibre optic detection system and (b) a photograph of a free space fibre fabricated in this study.

[21]. The most common detection methods used in conjunction with microfluidics are electrochemical such as amperometry [22–24] and optical such as absorbance [25] or chemiluminescence [26]. Optical components are typically fabricated from integrated waveguides and/or optical fibres [27–29]. However, the biggest challenges in the fabrication of optical components directly integrated into the LOC designs are the high cost, complex fabrication, low sensitivity, and bulky equipment. The use of DFR as microfluidic fabrication material can help solve these issues, and this has yet to be studied extensively.

In this work, we investigated the performance of free-space fibre optic detection in LOC for several microorganisms. The device consisted of two free-space multimode fibre pigtails for particle detection. This technology enables multimode fibre pigtails to be embedded into microfluidic for detection. The multimode fibre pigtails are aligned and sealed within microfabricated grooves perpendicular to the fluid channel.

2. Materials and Methods

2.1. Fabrication of LOC Devices. Fabrication of microfluidic integrated with fibre optic was based on already reported procedures using dry film resist [30, 31]. The design of the microfluidic channel is shown in Figure 1. The detection system is composed of two multimode pigtails which were connected to a UV-Vis spectrometer. The LOC system consisted of a single channel (4 cm length, 0.2 cm width, and an approximate height of 125 μm) and the detection reservoir having a 0.1 cm diameter. This chip was bonded with two multimode pigtails using UV glue. The detection could be employed as a part of the integrated LOC system as well as a single unit. In this study, we operated this detection unit as a separate chip.

2.2. Preparation of Microorganism. *E. coli* strains were grown overnight in Luria-Bertani (LB) Miller broth and on LB Miller agar at 37°C in a shaker with 150 rpm. After the inoculation process, the solution was transferred and centrifuged three times at 8,000 rpm for 3 min using a high-speed centrifuge. The supernatant was removed and replaced with distilled water after each centrifugation process. The centrifugation process was necessary to remove unwanted particle and to obtain a low and stable value of medium conductivity.

Dried yeast powder was used as the source of *S. cerevisiae* yeasts; 0.1 g of yeast powder was dissolved in 10 mL of distilled water (DI water) and kept in a water bath for 30 min to produce the live yeast solution. The live yeast solution was centrifuged at 8,000 rpm for 3 min using the high-speed centrifuge. The supernatant was discharged, and pallets were suspended by pipetting 10 mL of DI water.

Strains of *A. hydrophila* was grown on tryptic soy agar (TSA, Oxide), incubated overnight. The sample was harvested and washed using DI water by repeated centrifugation and replacement of the supernatant. The cells were centrifuged at 8,000 rpm for 3 min using the high-speed centrifuge. A concentrated cell suspension was then made by the addition of a small amount of deionized water.

2.3. Experiment Detail. The schematic diagram of the integrated LOC device is shown in Figure 2, with a spectrometer (*JAZ*, Ocean Optics, USA) as the light source and readout optics, syringe pump (Model MD-1001, Bioanalytical Systems Inc.), and a DFR microfluidic chip containing a multimode fibre optic. The spectrometer was connected to a personal computer and was controlled using the SpectraSuite program. The absorbance unit of distilled water was used as the reference point for microchannel reading. The sample was then injected to the microchannel through inlet tubing using a syringe pump. The absorbance spectra (AU) of the sample as a function of time for continuous wavelength were recorded for the different microorganisms.

2.4. Detection Limit. To test the detection limit, 10 mL of sample was taken from the nutrient broth solution and added into a bottle. It was then centrifuged and the supernatant was removed, and then 10 mL of distilled water was added into the bottle and centrifuged again twice. The sample was diluted several times to obtain the sample with different but lower concentrations. We used a control sample containing only deionized (DI) water as a reference. The

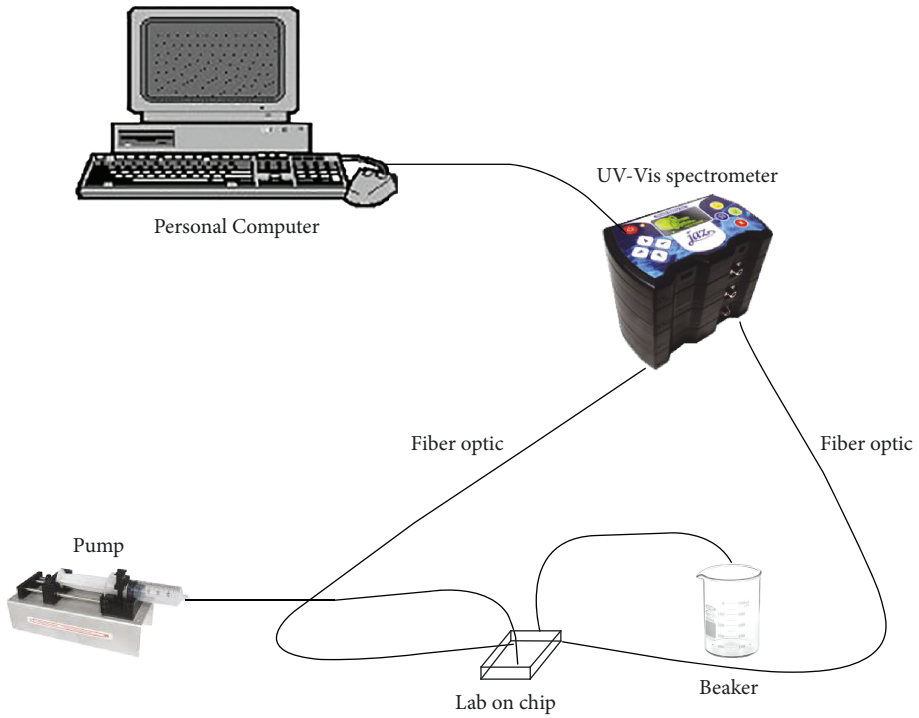

Figure 2: Experimental setup for lab-on-chip.

concentration of the samples prepared was determined using a hemocytometer.

2.5. Repeatability and Reproducibility. The repeatability of integrated LOC was measured in a dilution series of the sample, *E. coli* and *S. cerevisiae* for concentrations from 3.3×10^6 to 5.0×10^6 cells mL^{-1} and 1.1×10^8 to 2.1×10^8 cells mL^{-1}. Concentrations as low as 3.3×10^6 cells mL^{-1} and 1.1×10^8 cells mL^{-1} for *E. coli* and *S. cerevisiae*, respectively, were measured repeatedly after a day. Meanwhile, *A. hydrophila* concentration ranging from 4.1×10^6 to 6.7×10^6 cells mL^{-1} were demonstrated for repeatability experiment. The lowest concentration of *A. hydrophila* solution was measured repeatedly over the course of a day. Centrifugation was done for each concentration 3 times, and the supernatant was removed. Then, distilled water was added to each concentration.

2.6. Response Time. The method of sample preparation was similar to the reproducibility test. Different concentration samples for each species were prepared and used for the analysis of response time. Each concentration was centrifuged three times, and the supernatant was removed. After that, distilled water was added to each bottle to suspend the pallet.

3. Results and Discussion

3.1. Absorbance Spectra. Absorbance spectra of *E. coli* are plotted in Figure 3 to highlight the specific wavelength range. The observed absorbance spectra are typical for *E. coli*, and a significant peak can be seen from the absorbance spectrum of each concentration. It can be seen that *E. coli* cells absorbed

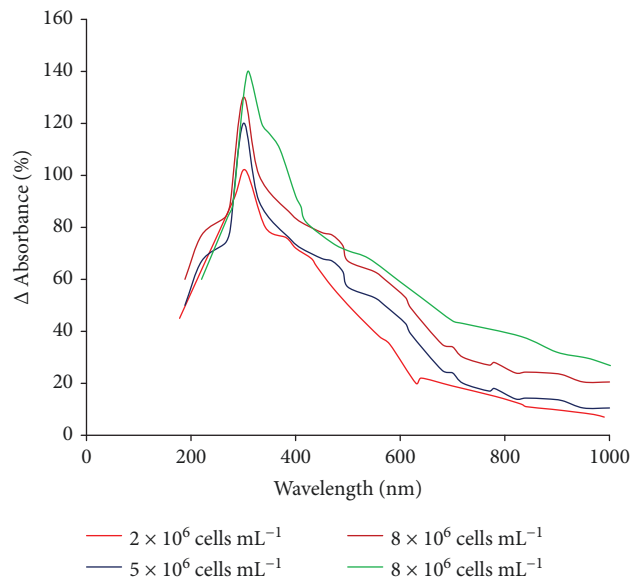

Figure 3: Absorbance spectra of *E. coli* in distilled water with different concentrations.

the wavelength at the range of 300–310 nm. These results support the previous research which showed a similar wavelength peak [32]. This outcome is contrary to that of Faghfuri et al. who found the wavelength to peak around 620 nm [33].

A graph of the absorbance spectra of different concentrations of *S. cerevisiae* is shown in Figure 4. The figure shows that the *S. cerevisiae* cells absorbed the wavelength at the range of 410-435 nm. These are typical absorbance spectra of *S. cerevisiae* cells and, in general, are different compared

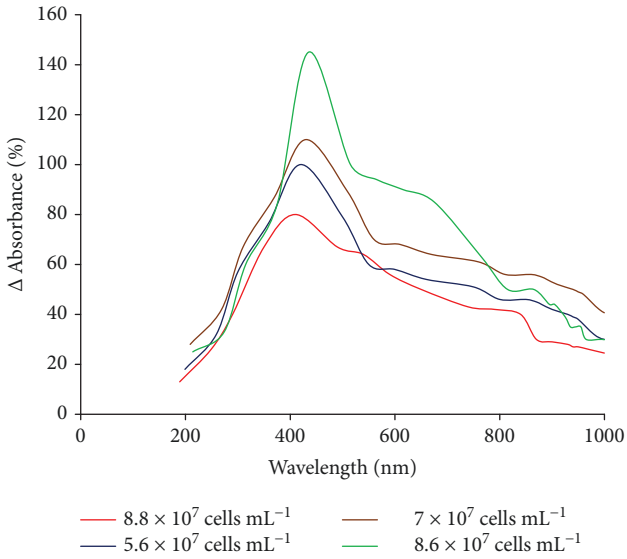

Figure 4: UV-Vis spectra of *S. cerevisiae* in distilled water with different concentrations.

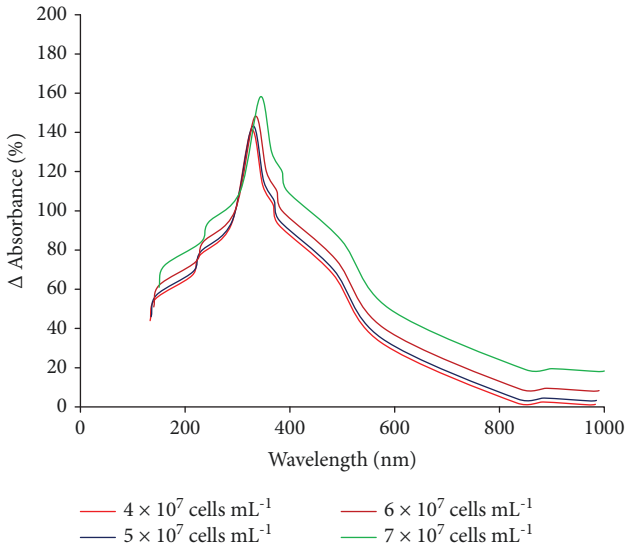

Figure 5: Absorbance spectra of *A. hydrophila* in distilled water with different concentrations.

to the trend observed previously for *E. coli* cells. The spectra are also similar to those observed in earlier studies, showing a wavelength peak for *S. cerevisiae* at 427 nm [34].

Figure 5 shows the graph of absorbance spectra against the wavelength for different concentrations of *A. hydrophila* cells. This is typical of absorbance spectra of *A. hydrophila*. Generally, it was seen that the absorbance peak increased with increasing absorbance. In view of the results obtained, *A. hydrophila* absorbed at the wavelength range of 325–345 nm. These results seem to be consistent with other researchers, which found the wavelength peak for *A. hydrophila* to be within this wavelength range [31, 35].

3.2. Detection Limit. The detection limit can be obtained when a further decrease in concentration does not cause a significant decrease in absorbance value. In this case, the detection limit is described in terms of the concentration of the microorganisms and is calculated according to the IUPAC recommendation [36]. From Figure 6, it is observed that below the concentration of 1.8×10^5 cells mL^{-1}, the absorbance value of *E. coli* cell did not show any considerable change. Further experiment was done for concentrations

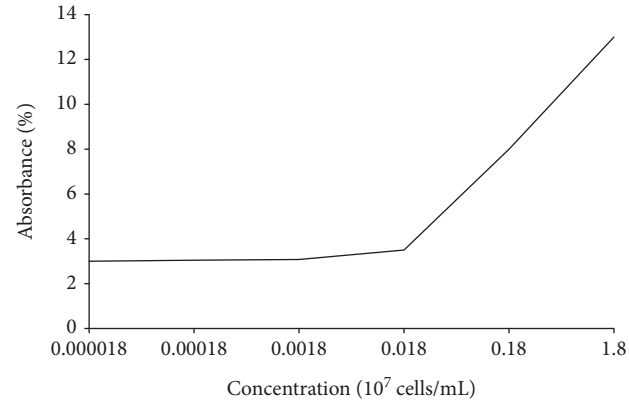

Figure 6: Peak absorbance value against concentration for *E. coli*.

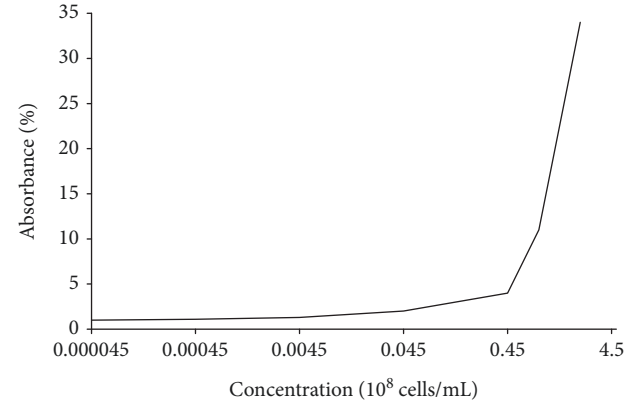

Figure 7: Peak absorbance value against concentration for *S. cerevisiae*.

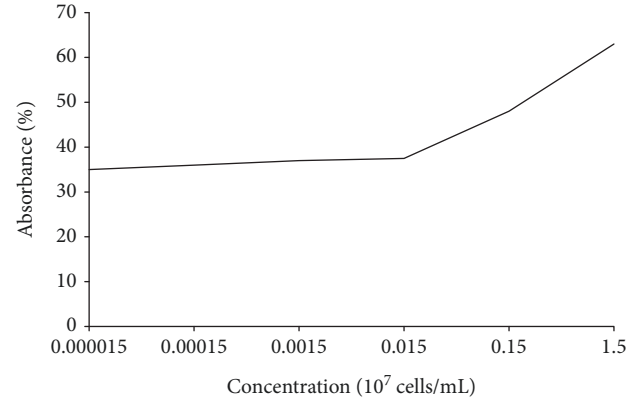

Figure 8: Peak absorbance value against concentration for *A. hydrophila*.

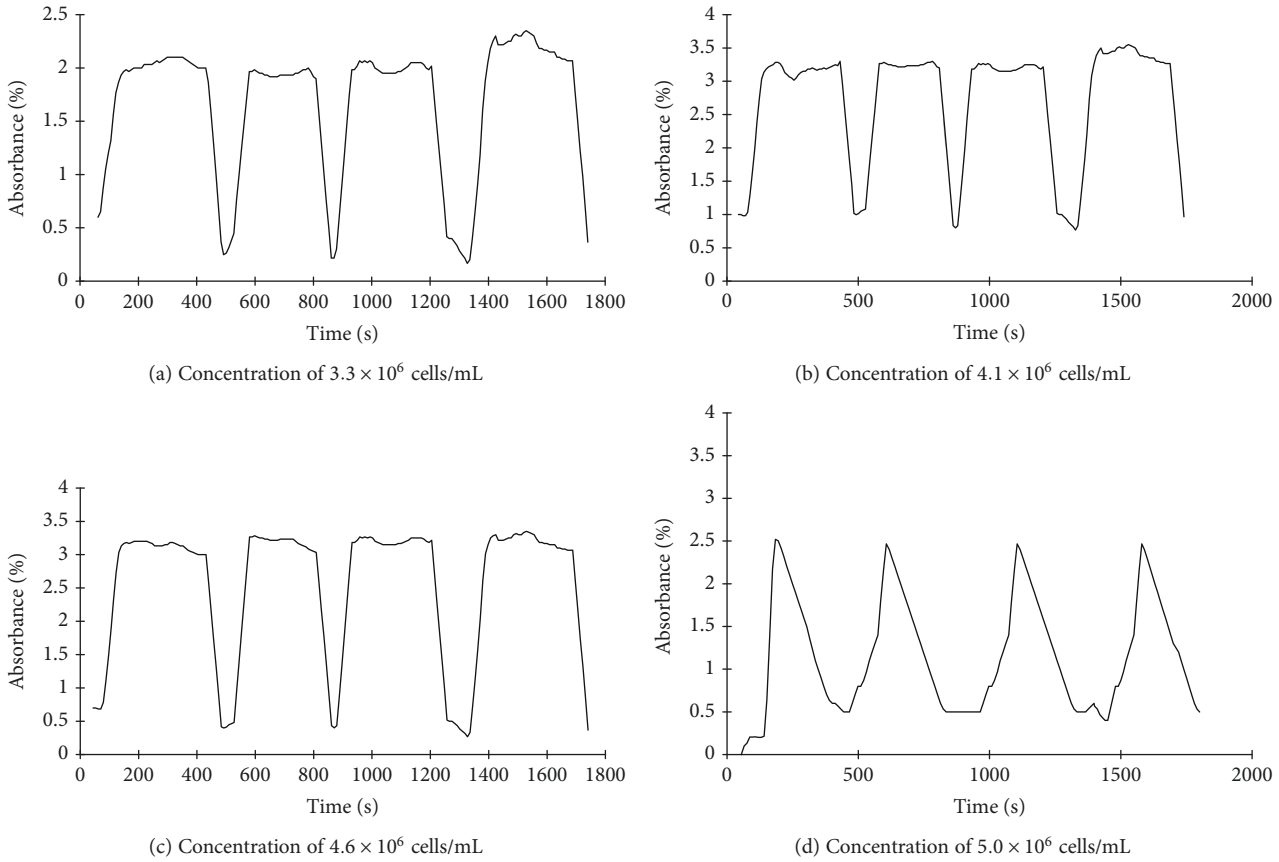

(a) Concentration of 3.3×10^6 cells/mL

(b) Concentration of 4.1×10^6 cells/mL

(c) Concentration of 4.6×10^6 cells/mL

(d) Concentration of 5.0×10^6 cells/mL

Figure 9: Graph of absorbance against time for *E. coli* at different concentrations.

between 5.0×10^4 cells mL^{-1} and 1.8×10^5 cells mL^{-1}, and no differences were observed. Hence, the detection limit of the microfluidic sensor towards *E. coli* is taken approximately as 1.0×10^5 cells mL^{-1}.

From Figure 7, it is observed that the difference in absorbance values of *S. cerevisiae* cells was small for concentrations between 4.5×10^3 cells mL^{-1} and 4.5×10^6 cells mL^{-1}, but notable differences were observed in absorbance values for concentrations greater than 4.5×10^6 cells mL^{-1}. Further experiment showed that the absorbance values within this range were very similar. Hence, the detection limit of the microfluidic device towards *S. cerevisiae* is taken to be at 1.0×10^6 cells mL^{-1}.

From Figure 8, it is observed that for *A. hydrophila*, the absorbance values did not show any notable changes when the concentration was decreased below 1.5×10^5 cells mL^{-1}. Further experiment was done to test the concentrations from 5.0×10^4 cells mL^{-1} to 1.5×10^5 cells mL^{-1}. The resulting absorbance values were similar. Hence, it is taken that the detection limit of the device towards *A. hydrophila* is at 1.0×10^5 cells mL^{-1}.

3.3. Repeatability and Reproducibility. Repeatability is the ability to produce duplicate measurement of the same sample under the same condition, while reproducibility is the ability to produce an identical measurement of the same sample at

Table 1: Standard deviation of the absorbance readings for *E. coli*.

Concentration (cells/mL)	Average of absorbance (%)	Standard deviation
3.3×10^6	1.7297	0.0607
4.1×10^6	3.0261	0.0772
4.6×10^6	3.1568	0.0244
5.0×10^6	2.5364	0.1864

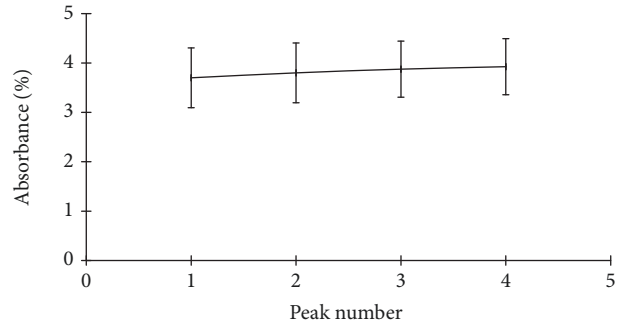

Figure 10: Standard deviation analysis for *E. coli* at 4.1×10^6 cells/mL.

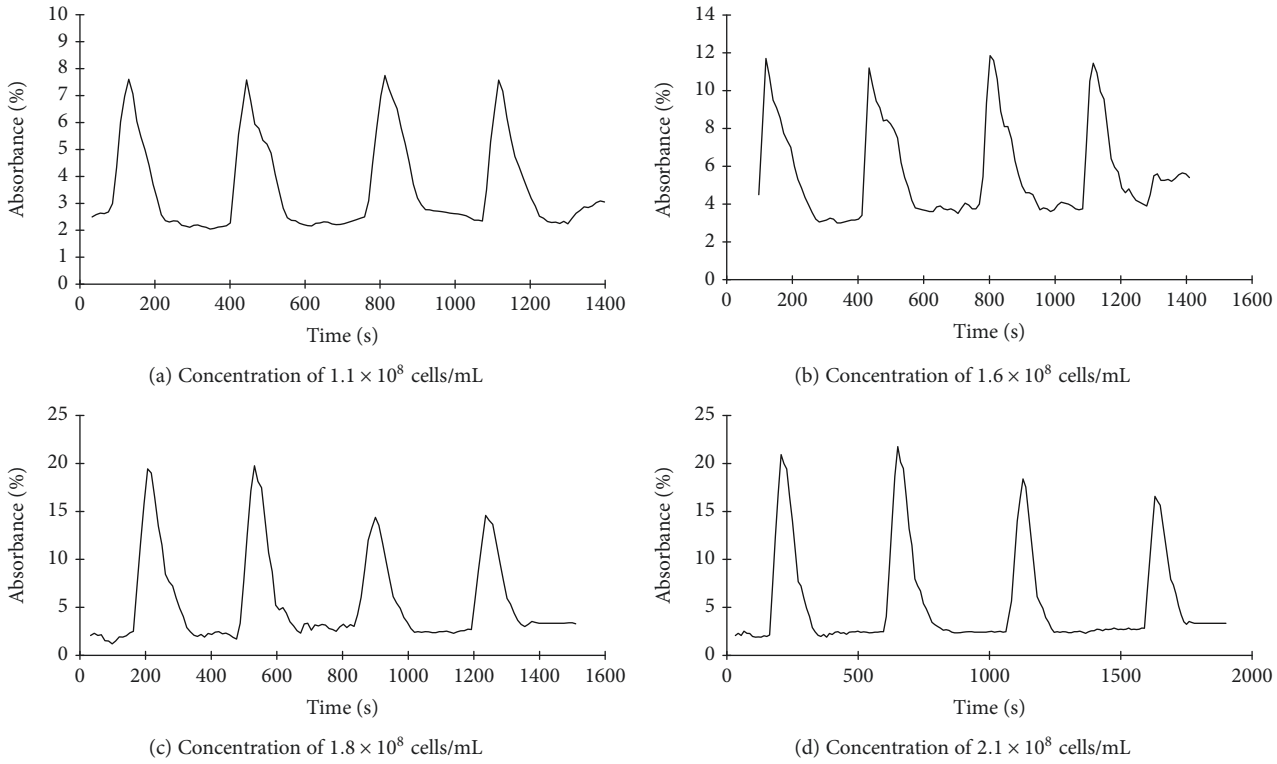

Figure 11: Graph of absorbance against time for *S. cerevisiae* at different concentrations.

different conditions. The repeatability and reproducibility tests are important in determining the precision of the readings obtained.

Figure 9 shows the graph of absorbance against time for different concentrations of *E. coli*. For each concentration, an equal volume of the sample is then immediately added to the microfluidic using a syringe pump. Table 1 shows the standard deviation of the absorbance values obtained for different concentrations of *E. coli*. There were little differences observed between each of the concentration as the standard deviation was less than 0.18. This indicates that the readings of absorbance are nearly the same for each concentration. As shown in Figure 9, the peak values are nearly the same for each concentration of *E. coli*. This represents good repeatability of the measurement.

The evaluation for *E. coli* is also repeated for the concentration of 4.1×10^6 cells mL^{-1} in another day. This experiment is aimed at examining the reproducibility of the microfluidic sensor towards *E. coli* species. Figure 10 shows the absorbance values with standard deviations generated for *E. coli*. Here, the standard deviations were calculated from the four peak absorbance measurements. Numbers of peaks refer to the number of a trial that corresponds to the maximum absorbance. The figure showed significant standard deviation in all the readings obtained for reproducibility experiment, which is believed to have resulted from microorganism die-off rates and produce by-products during storage [37]. This could be attributed to poor storage of microorganism and insufficient centrifugation process [38].

Table 2: Standard deviation of the absorbance readings for *S. cerevisiae*.

Concentration (cells/mL)	Average of absorbance (%)	Standard deviation
1.1×10^8	8.5803	0.2958
1.6×10^8	12.2880	0.2784
1.8×10^8	19.4313	1.4248
2.1×10^8	21.8488	1.1594

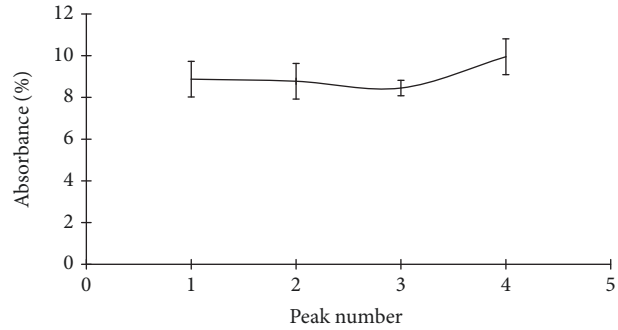

Figure 12: Error bar analysis for *S. cerevisiae* at 1.1×10^8 cells/mL.

The graph of absorbance against time for different concentrations of *S. cerevisiae* is shown in Figure 11. In these experiments, a similar volume of the sample was added and removed from the microfluidic channel using a syringe

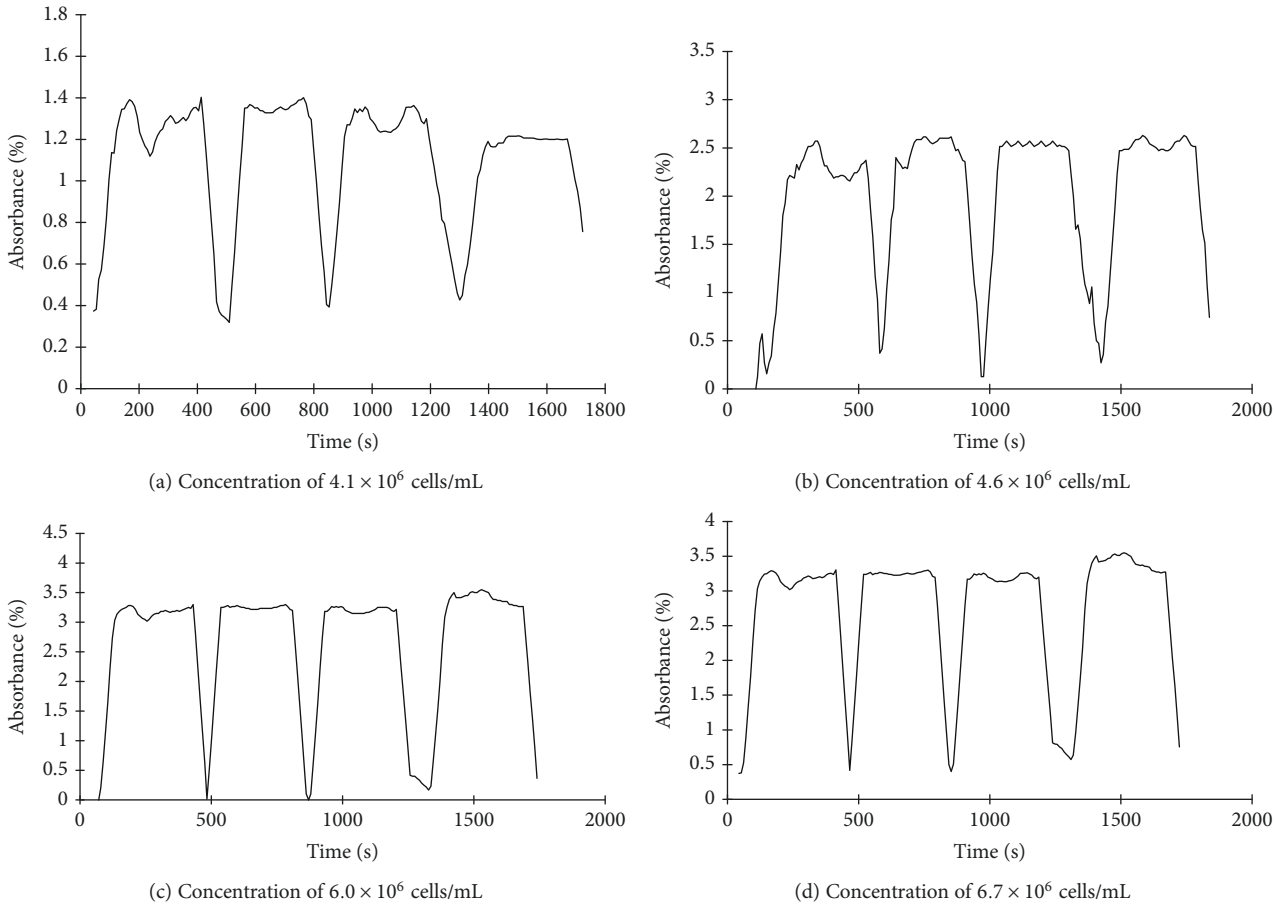

Figure 13: Graph of absorbance against time for *A. hydrophila* at different concentrations.

pump, as described in a previous experiment. Table 2 shows the standard deviation of the absorbance values obtained for different concentrations of *S. cerevisiae*. In comparison, the standard deviations for *S. cerevisiae* at different concentrations were greater than 1.0 and, therefore, greater than the standard deviation of *E. coli*. This significant discrepancy of peak values as shown in Figure 10 between *S. cerevisiae* and *E. coli* could be due to the size of microorganisms since *S. cerevisiae* (~8 micron) is bigger than *E. coli* (~1 micron). The results obtained were congruent with the previous work carried out by Sherman [39].

The evaluation for *S. cerevisiae* is also repeated for the concentration of 1.1×10^8 cells mL^{-1} in another day. The reproducibility test was carried out using a microfluidic sensor. The graph of absorbance against time is plotted in Figure 12. The results of the reproducibility analysis showed significant errors mainly due to die-off rates and produce by-products during storage as previously mentioned.

The graph of absorbance against time for four different concentrations of *A. hydrophila* is shown in Figure 13. For each concentration, the sample is added and removed from the microfluidic channel four times to observe the consistency of the peak absorbance value. Table 3 shows the standard deviation of the absorbance value obtained for different concentrations of *A. hydrophila*. In the view of the results obtained, the standard deviation for each of the concentration was lower than 0.11, indicating good repeatability of the result.

Table 3: Standard deviation of the absorbance readings for *A. hydrophila*.

Concentration (cells/mL)	Average of absorbance (%)	Standard deviation
4.1×10^6	1.1907	0.0656
4.6×10^6	2.5181	0.0748
6.0×10^6	3.2282	0.1015
6.7×10^6	2.9648	0.1169

The experiment is repeated for the concentration of 4.6×10^6 cells mL^{-1} in the next day. This was to examine the reproducibility of the microfluidic sensor towards the *A. hydrophila* species. The error bar graph of *A. hydrophila* is shown in Figure 14. A similar trend was observed in the error bar graph for all samples. The standard deviation of *A. hydrophila* increased when repeated with a similar concentration. This inconsistency may be due to inadequate periodic cleaning of microfluidic to prevent the residual cells from staying in the microfluidic. Hence, the flow rate

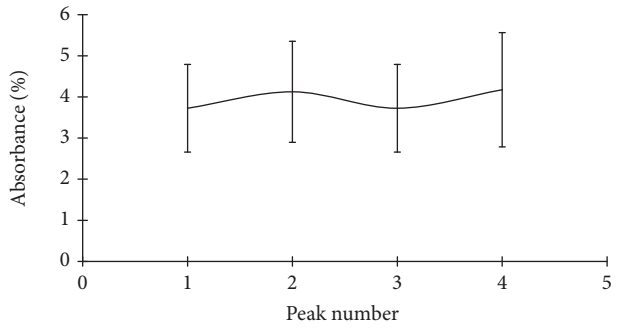

Figure 14: Error bar analysis for *A. hydrophila* at 4.6×10^6 cells/mL.

and absorbance measurement would be affected. Periodic cleaning must be incorporated as a preventive measure against clogging in LOC [40].

3.4. Response Time. Response time is the time taken for the sensor to change its output from its previous state to a value within a tolerance band of the new correct value such as 90% of the new correct value. For each species, four tests were performed with four different concentrations. These four tests are represented by four peaks on the graph of absorbance against time.

A graph of absorbance against time used to determine the response time for *E. coli* is depicted in Figure 15. The graph was generated using the data at the wavelength range of 310 ± 10 nm and the response time was taken from the lowest to the highest absorbance. From the data, it is apparent that the four readings of response time from the low to high concentration were 143 s, 107 s, 93 s, and 143 s. Therefore, the response time of the microfluidic sensor towards *E. coli* is determined by taking the average of these four readings, which was 122 s.

Figure 16 presents the graph of absorbance against time used to determine the response time for *S. cerevisiae*. The graph is generated using the data at the wavelength range of 435 ± 10 nm. The response times for *S. cerevisiae* are 93 s, 73 s, 65 s, and 80 s starting from the low concentration to the high concentration. Therefore, the average response time of the microfluidic sensor towards *S. cerevisiae* was 78 s.

The graph of absorbance against time at a wavelength of 343 ± 10 nm is presented in Figure 17 in order to determine the response time for *A. hydrophila*. From the graph, four readings of response time were, from low concentration to high concentration, 86 s, 87 s, 85 s, and 90 s. Therefore, the average response time of the microfluidic sensor towards *A. hydrophila* was 87 s.

This study has found that generally, the peak absorbance value increases when the concentration of the sample increases. There is an error that might come from the inconsistent flow rate and the time interval of adding samples to the microfluidic channel. The error is difficult to control as the sample was added to the channel manually. The average response time for all the samples was less than 2 minutes. Although the response time was generally higher than the results reported by other researchers [41, 42], the results were still acceptable because some of the performance criteria were found to be better than the average performance of the previous works, such as the detection limit, repeatability, response time, and sensitivity. Overall, the presented results showed that fibre optic detection used in this integrated LOC can be used for the purpose of microorganism sensing at a satisfactory rate.

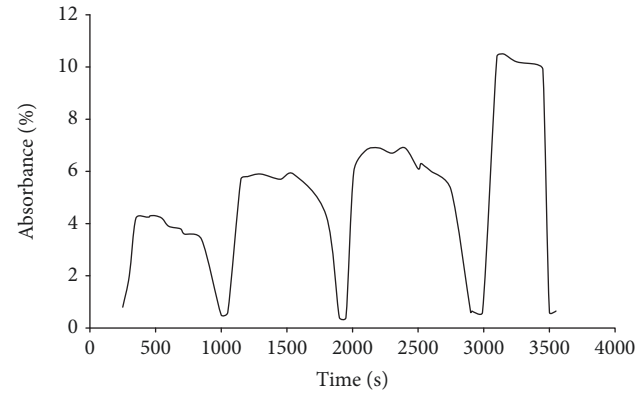

Figure 15: Dynamic response of *E. coli* for different concentrations.

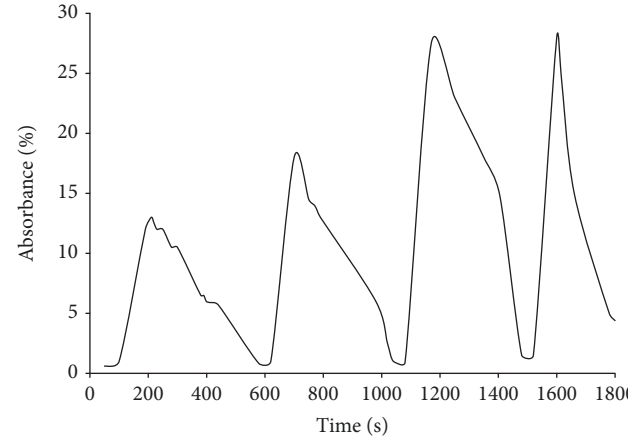

Figure 16: Dynamic response of *S. cerevisiae* for different concentrations.

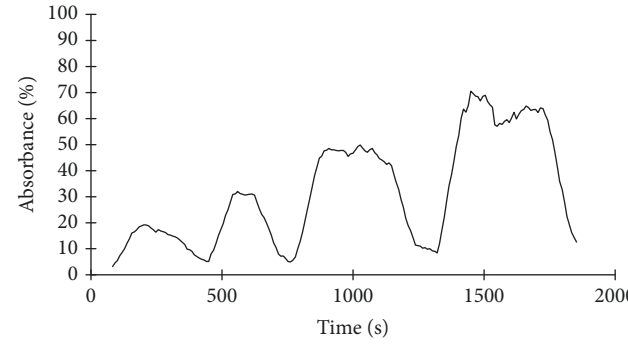

Figure 17: Dynamic response of *A. hydrophila* for different concentrations.

4. Conclusions

The fabrication of integrated LOC with optical detection was successfully demonstrated in this work. The detection of microorganisms is based on absorbance and performed in continuous-flow systems. The integrated LOC presented here offers a new approach in fabricating low-cost LOC, involving a less complex fabrication process and possible integration of multimode fibre optic without the need for a spliced fibre. In addition, the integration of optical detection avoids the need for expensive readout optics.

Data Availability

The data used to support the findings of this study are available from the corresponding author upon request.

Conflicts of Interest

The authors declare that there is no conflict of interest regarding the publication of this paper.

Acknowledgments

We would like to thank Malaysia Ministry of Science, Technology and Innovation for funding this project (SF-02-01-04-SF1214), Majlis Amanah Rakyat (MARA) for providing financial assistance, and Dr. Zalini Yunus for providing the assistance needed for this research.

References

[1] A. Chałupniak and A. Merkoçi, "Toward integrated detection and graphene-based removal of contaminants in a lab-on-a-chip platform," *Nano Research*, vol. 10, no. 7, pp. 2296–2310, 2017.

[2] M. Medina-Sánchez, S. Miserere, E. Morales-Narváez, and A. Merkoçi, "On-chip magneto-immunoassay for Alzheimer's biomarker electrochemical detection by using quantum dots as labels," *Biosensors and Bioelectronics*, vol. 54, pp. 279–284, 2014.

[3] S. L. Marasso, E. Giuri, G. Canavese et al., "A multilevel lab on chip platform for DNA analysis," *Biomedical Microdevices*, vol. 13, no. 1, pp. 19–27, 2011.

[4] S. Kurbanoglu, C. C. Mayorga-Martinez, M. Medina-Sánchez, L. Rivas, S. A. Ozkan, and A. Merkoçi, "Antithyroid drug detection using an enzyme cascade blocking in a nanoparticle-based lab-on-a-chip system," *Biosensors and Bioelectronics*, vol. 67, pp. 670–676, 2015.

[5] H. Kimura, T. Ikeda, H. Nakayama, Y. Sakai, and T. Fujii, "An on-chip small intestine–liver model for pharmacokinetic studies," *Journal of Laboratory Automation*, vol. 20, no. 3, pp. 265–273, 2015.

[6] J. Ozhikandathil, S. Badilescu, and M. Packirisamy, "Detection of bovine growth hormone using conventional and lab-on-a-chip technologies: a review," *International Journal of Advances in Engineering Sciences and Applied Mathematics*, vol. 7, no. 4, pp. 177–190, 2015.

[7] J. Ozhikandathil and M. Packirisamy, "Nano-islands integrated evanescence-based lab-on-a-chip on silica-on-silicon and polydimethylsiloxane hybrid platform for detection of recombinant growth hormone," *Biomicrofluidics*, vol. 6, no. 4, article 046501, 2012.

[8] A. Hasan, M. Nurunnabi, M. Morshed et al., "Recent advances in application of biosensors in tissue engineering," *BioMed Research International*, vol. 2014, Article ID 307519, 18 pages, 2014.

[9] L. Y. Yeo, H.-C. Chang, P. P. Y. Chan, and J. R. Friend, "Microfluidic devices for bioapplications," *Small*, vol. 7, no. 1, pp. 12–48, 2011.

[10] E. K. Sackmann, A. L. Fulton, and D. J. Beebe, "The present and future role of microfluidics in biomedical research," *Nature*, vol. 507, no. 7491, pp. 181–189, 2014.

[11] M. Smolka, D. Puchberger-Enengl, M. Bipoun et al., "A mobile lab-on-a-chip device for on-site soil nutrient analysis," *Precision Agriculture*, vol. 18, no. 2, pp. 152–168, 2017.

[12] A. M. Kaushik, K. Hsieh, and T.-H. Wang, "Droplet microfluidics for high-sensitivity and high-throughput detection and screening of disease biomarkers," *Wiley Interdisciplinary Reviews: Nanomedicine and Nanobiotechnology*, vol. 10, no. 6, article e1522, 2018.

[13] M. Medina-Sánchez, M. Cadevall, J. Ros, and A. Merkoçi, "Eco-friendly electrochemical lab-on-paper for heavy metal detection," *Analytical and Bioanalytical Chemistry*, vol. 407, no. 28, pp. 8445–8449, 2015.

[14] E. T. da Costa, M. F. S. Santos, H. Jiao, C. L. do Lago, I. G. R. Gutz, and C. D. Garcia, "Fast production of microfluidic devices by CO2 laser engraving of wax-coated glass slides," *Electrophoresis*, vol. 37, no. 12, pp. 1691–1695, 2016.

[15] A. Ambrosi, M. Guix, and A. Merkoçi, "Magnetic and electrokinetic manipulations on a microchip device for bead-based immunosensing applications," *Electrophoresis*, vol. 32, no. 8, pp. 861–869, 2011.

[16] M. Medina-Sánchez, S. Miserere, and A. Merkoçi, "Nanomaterials and lab-on-a-chip technologies," *Lab on a Chip*, vol. 12, no. 11, pp. 1932–1943, 2012.

[17] A. Ayoib, U. Hashim, M. K. M. Arshad, and V. Thivina, "Soft lithography of microfluidics channels using su-8 mould on glass substrate for low cost fabrication," in *2016 IEEE EMBS Conference on Biomedical Engineering and Sciences (IECBES)*, pp. 226–229, Malaysia, December 2016.

[18] O. D. Pessoa-Neto, V. B. dos Santos, F. C. Vicentini et al., "A low-cost automated flow analyzer based on low temperature co-fired ceramic and LED photometer for ascorbic acid determination," *Central European Journal of Chemistry*, vol. 12, no. 3, pp. 341–347, 2014.

[19] P. Couceiro, S. Gómez-de Pedro, and J. Alonso-Chamarro, "All-ceramic analytical microsystems with monolithically integrated optical detection microflow cells," *Microfluidics and Nanofluidics*, vol. 18, no. 4, pp. 649–656, 2015.

[20] P. Frank, S. Haefner, G. Paschew, and A. Richter, "Rounding of negative dry film resist by diffusive backside exposure creating rounded channels for pneumatic membrane valves," *Micromachines*, vol. 6, no. 11, pp. 1588–1596, 2015.

[21] J. Wu, M. Dong, S. Santos, C. Rigatto, Y. Liu, and F. Lin, "Lab-on-a-chip platforms for detection of cardiovascular disease and cancer biomarkers," *Sensors*, vol. 17, no. 12, p. 2934, 2017.

[22] Y. Zhao, X. Fang, X. Yan et al., "Nanorod arrays composed of zinc oxide modified with gold nanoparticles and glucose oxidase for enzymatic sensing of glucose," *Microchimica Acta*, vol. 182, no. 3-4, pp. 605–610, 2015.

[23] B. V. Chikkaveeraiah, V. Mani, V. Patel, J. S. Gutkind, and J. F. Rusling, "Microfluidic electrochemical immunoarray for ultrasensitive detection of two cancer biomarker proteins in serum," *Biosensors and Bioelectronics*, vol. 26, no. 11, pp. 4477–4483, 2011.

[24] P. M. Misun, J. Rothe, Y. R. F. Schmid, A. Hierlemann, and O. Frey, "Multi-analyte biosensor interface for real-time monitoring of 3D microtissue spheroids in hanging-drop networks," *Microsystems & Nanoengineering*, vol. 2, no. 1, article 16022, 2016.

[25] S.-u. Hassan, A. M. Nightingale, and X. Niu, "Continuous measurement of enzymatic kinetics in droplet flow for point-of-care monitoring," *Analyst*, vol. 141, no. 11, pp. 3266–3273, 2016.

[26] E. Lebiga, R. Edwin Fernandez, and A. Beskok, "Confined chemiluminescence detection of nanomolar levels of H2O2in a paper–plastic disposable microfluidic device using a smartphone," *Analyst*, vol. 140, no. 15, pp. 5006–5011, 2015.

[27] Y.'n. Wang, Y. Luo, B. Xiong et al., "A simple fabrication process for SiNx/SiO2waveguide based on sidewall oxidation of patterned silicon substrate," *Journal of Modern Optics*, vol. 64, no. 3, pp. 226–230, 2016.

[28] A. Chandrasekaran and M. Packirisamy, "Integrated microfluidic biophotonic chip for laser induced fluorescence detection," *Biomedical Microdevices*, vol. 12, no. 5, pp. 923–933, 2010.

[29] Y. Xin, G. Pandraud, A. van Langen-Suurling, and P. French, "Tapered SU8 waveguide for evanescent sensing by single-step fabrication," in *2017 IEEE Sensors*, pp. 1–3, Scotland, October 2017.

[30] F. Kamuri, Z. Z. Abidin, N. A. M. Yunus et al., "Optimization on the preparation of microfluidic channel using dry film resist," in *2015 International Conference on Smart Sensors and Application (ICSSA)*, pp. 11–15, Malaysia, May 2015.

[31] S. Gauri, Z. Z. Abidin, M. F. Kamuri, M. A. Mahdi, and N. A. M. Yunus, "Detection of Aeromonas hydrophila using fiber optic microchannel sensor," *Journal of Sensors*, vol. 2017, Article ID 8365189, 10 pages, 2017.

[32] R. Bharadwaj, V. V. R. Sai, K. Thakare et al., "Evanescent wave absorbance based fiber optic biosensor for label-free detection of E. coli at 280nm wavelength," *Biosensors and Bioelectronics*, vol. 26, no. 7, pp. 3367–3370, 2011.

[33] E. Faghfuri, J. Fooladi, S. Sepehr, and S. Z. Moosavi-Nejad, "L-Tryptophan production by whole cells of Escherichia coli based on Iranian sugar beet molasses," *Jundishapur Journal of Microbiology*, vol. 6, no. 4, 2013.

[34] M. Bercu, X. Zhou, A. C. Lee, D. P. Poenar, C. K. Heng, and S. N. Tan, "Spectral characterization of yeast cells with an epitaxy-based UV-Vis optical sensor," *Biomedical Microdevices*, vol. 8, no. 2, pp. 177–185, 2006.

[35] G. P. Richards and M. A. Watson, "A simple fluorogenic method to detect Vibrio cholerae and Aeromonas hydrophila in well water for areas impacted by catastrophic disasters," *The American Journal of Tropical Medicine and Hygiene*, vol. 75, no. 3, pp. 516–521, 2006.

[36] J. Sanchez, "Estimating detection limits in chromatography from calibration data: ordinary least squares regression vs. weighted least squares," *Separations*, vol. 5, no. 4, p. 49, 2018.

[37] R. P. S. Suri, H. M. Thornton, and M. Muruganandham, "Disinfection of water using Pt- and Ag-doped TiO2 photocatalysts," *Environmental Technology*, vol. 33, no. 14, pp. 1651–1659, 2012.

[38] S. H. Van Ierssel, E. M. Van Craenenbroeck, V. M. Conraads et al., "Flow cytometric detection of endothelial microparticles (EMP): effects of centrifugation and storage alter with the phenotype studied," *Thrombosis Research*, vol. 125, no. 4, pp. 332–339, 2010.

[39] F. Sherman, "Getting started with yeast," in *Methods in Enzymology*, vol. 350, pp. 3–41, Academic Press, 2002.

[40] L. W. Jang, M. E. Razu, E. C. Jensen, H. Jiao, and J. Kim, "A fully automated microfluidic micellar electrokinetic chromatography analyzer for organic compound detection," *Lab on a Chip*, vol. 16, no. 18, pp. 3558–3564, 2016.

[41] A. Ymeti, J. S. Kanger, J. Greve et al., "Integration of microfluidics with a four-channel integrated optical Young interferometer immunosensor," *Biosensors and Bioelectronics*, vol. 20, no. 7, pp. 1417–1421, 2005.

[42] S. Lee, J. Park, H. Im, and H. Jung, "A microfluidic ATP-bioluminescence sensor for the detection of airborne microbes," *Sensors and Actuators B: Chemical*, vol. 132, no. 2, pp. 443–448, 2008.